SLEEPJ, 2019, 1–14

doi: 10.1093/sleep/zsz184
Advance Access Publication Date: 2 August 2019
Original article

ORIGINAL ARTICLE

Evidence for sleep-dependent synaptic renormalization in mouse pups

Luisa de Vivo[1,2,†], Hirotaka Nagai[1,3,†], Noemi De Wispelaere[1,‡], Giovanna Maria Spano[1,‡], William Marshall[1,4], Michele Bellesi[1,2], Kelsey Marie Nemec[1], Shannon Sandra Schiereck[1], Midori Nagai[1,3], Giulio Tononi[1,*] and Chiara Cirelli[1,*]

[1]Department of Psychiatry, University of Wisconsin-Madison, 6001 Research Park Blvd, Madison, WI 53719, [2]Present address: School of Physiology, Pharmacology & Neuroscience, University of Bristol, Bristol BS8 1TD, UK, [3]Present address: Division of Pharmacology, School of Medicine, Kobe University, Kobe, Japan and [4]Present address: Department of Mathematics and Statistics, Brock University, St. Catharines, ON, L2S 3A1, Canada

[†]Co-first authors.

[‡]Co-second authors.

*Corresponding author. Chiara Cirelli, Department of Psychiatry, University of Wisconsin – Madison, 6001 Research Park Blvd, Madison, WI 53719. Email: ccirelli@wisc.edu. Giulio Tononi, Department of Psychiatry, University of Wisconsin – Madison, 6001 Research Park Blvd, Madison, WI 53719. Email: gtononi@wisc.edu.

Abstract

In adolescent and adult brains several molecular, electrophysiological, and ultrastructural measures of synaptic strength are higher after wake than after sleep [1, 2]. These results support the proposal that a core function of sleep is to renormalize the increase in synaptic strength associated with ongoing learning during wake, to reestablish cellular homeostasis and avoid runaway potentiation, synaptic saturation, and memory interference [2, 3]. Before adolescence however, when the brain is still growing and many new synapses are forming, sleep is widely believed to promote synapse formation and growth. To assess the role of sleep on synapses early in life, we studied 2-week-old mouse pups (both sexes) whose brain is still undergoing significant developmental changes, but in which sleep and wake are easy to recognize. In two strains (CD-1, YFP-H) we found that pups spend ~50% of the day asleep and show an immediate increase in total sleep duration after a few hours of enforced wake, indicative of sleep homeostasis. In YFP-H pups we then used serial block-face electron microscopy to examine whether the axon-spine interface (ASI), an ultrastructural marker of synaptic strength, changes between wake and sleep. We found that the ASI of cortical synapses (layer 2, motor cortex) was on average 33.9% smaller after sleep relative to after extended wake and the differences between conditions were consistent with multiplicative scaling. Thus, the need for sleep-dependent synaptic renormalization may apply also to the young, pre-weaned cerebral cortex, at least in the superficial layers of the primary motor area.

Significance Statement

In the mature brain several measures of synaptic strength increase with wake and decline with sleep, in line with the hypothesis that waking mainly strengthens synaptic connections due to ongoing learning, and sleep allows broad synaptic renormalization, reducing energy costs and preventing synaptic saturation. It is unknown whether the same changes occur during development, when the brain is still growing. By using serial electron microscopy to assess an ultrastructural measure of synaptic strength we find that in the primary motor cortex of 2-week-old mouse pups synapses are larger after sustained wake than after sleep, and changes are greater and more widespread than in older mice. This suggests that broad sleep-dependent synaptic renormalization occurs also in the pre-weaned brain.

Key words: sleep; cerebral cortex; serial electron microscopy; synapse

Submitted: 7 November, 2018; **Revised:** 13 June, 2019

Introduction

It has been hypothesized that waking should be associated with net synaptic strengthening in many brain circuits due to ongoing learning, and that sleep may mediate synaptic renormalization with several benefits both at the cellular and the systems level [3]. For example, stronger synapses require more energy and cellular supplies, calling for means to ensure synaptic homeostasis and cellular restoration. Moreover, a progressive increase in synaptic strength, if left unchecked, leads to runaway potentiation, decrease in signal-to-noise ratio, and impaired learning due to saturation, thereby impairing memory acquisition and consolidation. According to this synaptic homeostasis hypothesis (SHY), a core function of sleep would be to restore the brain at a time when it is disconnected from the environment, allowing neural circuits to be broadly reactivated in an off-line mode and to undergo a comprehensive and yet specific synaptic down-selection [3]. This hypothesis about sleep function has so far been supported by studies in adolescent and adult rodents as well as in humans, employing various complementary approaches to assess synaptic strength [1–3]. For instance, protein levels of GluA1-containing AMPA receptors measured in synaptoneurosomes of adult rats are higher after wake than after sleep across the entire cerebral cortex and hippocampus [4]. Electrophysiological markers of synaptic efficacy, such as the slope of cortical evoked responses, also increase broadly after wake and decrease after sleep in adult rats [4] and humans [5]. Other recent experiments found that specific patterns of neural activity during sleep are required for sleep-dependent down-selection of neural activity and synaptic strength, including cortical slow waves [6] and hippocampal sharp waves/ripples [7]. Recent studies also identified specific molecules involved in sleep-dependent synaptic weakening [8, 9].

Perhaps the most stringent prediction of SHY is that, since stronger synapses are larger [10], one should observe a net change in average synaptic size between wake and sleep, in a matter of a few hours. We recently tested this idea in primary motor and primary sensory cortex of adolescent mice using serial block-face electron microscopy (SBEM), to obtain direct, high-resolution 3D volume measurements of synaptic size during the sleep/waking cycle in ~ 7000 synapses [11]. In line with SHY, the axon-spine interface (ASI), the direct area of contact between pre-synapse and post-synapse, decreased on average by 18% after 6–8 hours of sleep as compared to 6–8 hours of wake, independent of whether mice were awake during the day or the night [11]. Sleep-dependent synaptic renormalization was found in small and medium size synapses, which together account for the majority (~80%) of all synapses, but not in the largest synapses. Before adolescence, however, when the brain is still growing and many new synapses are forming (reviewed in [12]) sleep is widely believed to promote synapse formation and growth [13–20]. During these developmental periods, therefore, synaptic renormalization has been considered an unlikely key function of sleep [21]. On the other hand, it is possible that the massive, fast-paced formation of new synapses during early development may pose even greater challenges to synaptic homeostasis than the increase in synaptic strength that occurs during wake in older animals [22]. To start addressing this question in this study we asked whether the growing and shrinking of synapses during wake and sleep, which we documented in the adolescent brain, also occur during early development, when both sleep and synaptic remodeling are prominent [12]. We focused on 2-week-old mouse pups because their brain is still undergoing significant developmental changes and periods of sleep and wake can reliably be detected using chronic, noninvasive behavioral analysis.

Methods

All animal procedures and experimental protocols followed the National Institutes of Health Guide for the Care and Use of Laboratory Animals [23] and were approved by the licensing committee. All animal facilities were reviewed and approved by the institutional animal care and use committee (IACUC) of the University of Wisconsin-Madison, and were inspected and accredited by association for assessment and accreditation of laboratory animal care (AAALAC).

Behavioral experiments

Sleep/wake behavioral analysis in CD-1 mice.

Six CD-1 female pregnant mice were obtained from Jackson Laboratory and maintained in a colony room, in standard laboratory cages, on a 12 hour light/12 hour dark cycle (lights on at 8 am) with free access to water and food available ad libitum. The CD-1 strain was selected for the initial sleep/wake analysis because the white fur of these animals made behavioral scoring possible also under red light conditions at night. Mice were inspected every day for new pups. Postnatal day 0 (P0) was defined as the day of birth. Four days before the experiment litters were culled to two pups per litter (either sex), moved in the recording chamber (one chamber/ litter), and given a few days of habituation. At P13, mice were randomly assigned to two experimental groups: in the baseline group 3 litters (six pups) and their dams were left undisturbed and their behavior was recorded for 24 hours starting at 8 pm using a digital high definition camera. In the second group 3 litters (six pups) and their dams were forced to be awake for 6 hours starting at 2 pm using gentle handling and by introducing novel objects in the cage anytime that they attempted to fall asleep, and then left undisturbed and video-recorded for the following 24 hours of recovery. Before starting the experiment, the fur on the back of the pups and the tail were labeled using nontoxic permanent markers to facilitate pup identification during the analysis.

Behavior was scored offline by a single operator blind to the experimental condition, using behavioral criteria previously established in rats [24–28]. The scoring was based on 30-second epochs because previous EEG analysis in pups (both rats and mice) showed that the mean episode duration for wake, quiet sleep and active sleep is at least 30 seconds after P12 [27, 29]. Since in contrast to previous studies the experiments were conducted before weaning, two additional criteria—visibility and position—were used to better characterize behavioral states. The visibility of the pup was scored as 0 (no visibility), 1 (partial visibility), 2 (full visibility), because often pups laid on their back under the dam while they were eating. An epoch was scored as visible (partial) even if the entire body was not in clear view, because tail and/or hind limbs were informative enough to establish the behavioral state. Overall, less than 3% of the data (~42 minutes/24 hours) could not be scored (no visibility), with no difference between baseline group and recovery group (mean

± SEM in minutes across 24 hours, baseline = 42.5 ± 7.1; recovery = 41.2 ± 9.4; t-test $p = 0.92$). Epochs with no visibility were not used for analysis and Figure 2. The second added criterion, the position of the pup relative to the dam or to the other sibling, was used to distinguish between spontaneous or evoked awakenings (see below). The position was scored as 0 (pup alone), 1 (pup with other sibling), 2 (pup with dam in nursing position), 3 (pup with dam in other positions).

Five waking activities were distinguished: (1) exploring, including walking, running, climbing, jumping, sniffing and digging; (2) grooming, including active grooming, social grooming and passive grooming, i.e. time spent being groomed by the mother; (3) pre-eating/playing, defined as the time spent by the pup looking for the right position to be fed or, more rarely, the time spent playing in the presence of the mother; (4) eating, mostly by being nursed by the dam (this category also included any attempt by the pups to eat food pellets available in the cage, although it was unclear whether there was actual food intake); and (5) quiet waking, during which pups were not moving but had eyes open, or when eyes were closed but there was no muscle atonia, twitching or quivering.

Sleep was defined as a period of more than 15 seconds of immobility in which signs of decreased muscle tone were visible, such as the gradual fall of the tail or the relaxation of the hind limbs. When twitching and/or quivering of the extremities and/or whiskers could be observed, sleep was scored as active sleep (see videos in Supplementary Material, for examples). Conversely, episodes of sleep without any twitching or quivering were defined as quiet sleep, according to previously established criteria [27, 28]. During sleep the pups often woke up for short bouts of less than 15 seconds, consistent with results in adult rodents [30], and these events were scored as brief arousals. We distinguished between spontaneous and evoked awakenings and the latter were used to assess arousal threshold without actively interfering with the pups' behavior. Specifically, we computed the total amount of "disturbed" and "undisturbed" sleep, scoring a sleep epoch as disturbed if a sleeping pup was nudged by the sibling or the dam. When this brief disturbance awoke the pup we called the awakening "evoked". The behavior of the dam was scored using visibility (scored as explained above) and behavioral state (active or quiet waking or sleep).

Sleep/wake behavioral analysis in YFP-H mice

B6.Cg-Tg(Thy1-YFP)16Jrs/J mice (YFP-H, Jackson laboratory) were previously used to perform SBEM studies in the cerebral cortex at P30 [11, 31, 32] and developmental changes in sleep patterns during adolescence are well characterized in this strain [33]. Sleep/wake behavioral analysis in YFP-H pups was performed according to the same general criteria used for CD-1 mice, but with some differences. First, the analysis was restricted to the light phase because the dark fur of these mice made the behavioral scoring at night too difficult and unreliable. Second, because at 2 weeks of age these pups are significantly smaller than CD-1 pups (~25% smaller), the number of epochs that could not be scored (no visibility) was ~15%, higher than in CD-1 pups, but it did not differ before and after sleep deprivation (mean ± SEM in minutes in the last 8 hours of the light phase, baseline = 69.0 ± 27.2; recovery = 72.0 ± 21.0; t-test $p = 0.88$). Third, we did not try to distinguish between active and quiet sleep, and between disturbed and undisturbed sleep. Fourth, sleep deprivation was performed starting at light onset, to match the experimental design used in the ultrastructural experiments (see below).

Additional experiments were performed in other YFP-H pups to assess potential changes in body weight caused by sleep deprivation. At P13, YFP-H pups ($n = 10$) were kept with the dam and deprived of sleep for up to 8 hours starting at light onset. Pups were weighted at light onset and after 4 and 8 hours of sleep loss.

Ultrastructural experiments

Animals and experimental groups

As in a previous study in P30 mice [11], B6.Cg-Tg(Thy1-YFP)16Jrs/J mice were used (YFP-H). The litter and the dam were housed together in environmentally controlled recording chambers with free access to food and water (12 hours:12 hours light-dark cycle; lights on at 8 am). Litters were not culled (both sexes were used). Starting 1–2 days before the experiment a running wheel and 1–2 novel objects were introduced in the recording chamber at the beginning of each dark period, to ensure enriched housing conditions and facilitate the light/dark entrainment of the rest/activity cycle. The day of the experiment (P13) litters were randomly assigned to each experimental group. Since it was impossible to sleep deprive some pups without disturbing their siblings, the entire litter housed with the dam was either allowed to sleep or kept awake. In our previous study in P30 mice we measured synapse size and number after sleep, spontaneous wake at night, and forced wake during the day, focusing on layer 2 of primary motor and primary sensory cortex [11]. Since results in P30 mice did not differ between areas, in the current study we focused on layer 2 of primary motor cortex. In P30 mice we also found an almost identical increase (~18%) of ASI in both wake groups (spontaneous wake and enforced wake [EW]) relative to sleep. Because 2-week-old CD-1 pups were never spontaneously awake for several hours at night, and YFP-H pups could not be scored reliably in the dark, in the current study we did not have a spontaneous wake group at night. At light onset (8 am) pups were either allowed to sleep for 4.5 to 6 hours (S group) or kept awake as much as possible for the same period of time using gentle handling and novel objects (enforced wake, EW group). The time varied because it took ~1.5 hours to perfuse the entire litter, comprising 6–7 pups. Mice were killed in order based on their weight, from the smallest to the biggest pup. The same operators (L.dV., M.B.) perfused all pups.

Tissue preparation for electron microscopy

Methods were as previously described [11] and as before, blocks of tissue (1 mm^2) encompassing the primary motor cortex (M1, 1.85 mm anterior to bregma, 1.5 mm lateral) were stained blind to experimental condition.

Image acquisition

As previously described [11], serial images were obtained using a ΣIGMA VP field emission scanning electron microscope (Carl Zeiss NTS Ltd) equipped with 3View technology (Gatan Inc.) and a backscattered electron detector (aperture of 30 μm, high vacuum, acceleration voltage of 1.5–2 kV, image size of 5000 by 5000 pixels, image resolution in the xy plane of 4 nm). Nominal thickness of the ultrathin sections was 40–50 nm. Stacks of ~500

images each were acquired per mouse (~10 000–21 000 μm³) in layer 2 of M1, as in the previous study in P30 mice [11]. Images were Gaussian filtered and automatically aligned using the open source software Fiji [34]. Average actual section thickness for each stack was estimated using the cylindrical diameters method as previously described [35], and was comparable across conditions (mean ± std, S group = 49.2 ± 1.57 nm; EW group = 51.82 ± 3.18 nm). Dendritic segments and all their protrusions were segmented manually in TrakEM2 [36] by trained annotators who were blind to experimental condition. We randomly selected spiny dendritic segments whose diameter ranged between 0.47 and 1.01 μm. Densely spiny dendrites located in layer 2 include intermediate and terminal dendrites of layer 3 and 5 pyramidal neurons, as well as basal and oblique dendrites of layer 2 pyramidal neurons [37, 38]. The dendrites of some non pyramidal inhibitory neurons in layer 2, Martinotti cells, are also spiny, but their spine density is at least one-third lower than in pyramidal neurons [39]. To focus on pyramidal cells we therefore excluded dendritic segments with few or no spines, as well as dendrites with few spines and whose number of shaft synapses exceeded the number of spine synapses. Overall, in both groups less than 2% of dendrites were excluded from the analysis.

As before [11] all protrusions were defined as "spines" (in agreement with [10]), and distinguished in spines with or without synapses. Criteria to define a synapse included the presence of a presynaptic bouton with at least 1–2 synaptic vesicles within a 50 nm distance from the cellular membrane facing the spine, a visible synaptic cleft and a post-synaptic density. Spines without synapses represented 27.3% of all protrusions (Table 2). In total, 136 dendritic branches were segmented (5 mice/group, 10–18 dendrites/mouse). Distribution of dendritic diameters was balanced across experimental groups (p = 0.2722) and all segmentation data were tested for accuracy and consistency by the same experienced tracer (CC).

As before [11] the ASI was used as the ultrastructural measure of synaptic strength and traced at the interface between the spine head and the presynaptic terminal or bouton. Specifically, the region of contact between the two apposed objects was outlined in each individual section using the arealist brush suitably set at 1 pixel size. In this way, a quasi two-dimensional sheet-like object representing the interfaced region was created along the z dimension. The total surface area was calculated by computing the smoothed upper bound surface, according to the formula

$$\text{Smoothed upper bound surface} = \sum_{k=0}^{n} \left(P_s(a) \times \frac{1}{2}T\right) + \left(P_s(b) \times \frac{1}{2}T\right) + [A(a) - A(b)]$$

where n is the number of sections, a and b are the traced elements at the top and bottom of a section k of thickness T, P_s is the smoothed perimeter, and A is the area [36]. Finally, the areas of the traced element in the section $k = 1$ and in the section $k = n$ were subtracted from the smoothed upper bound surface value and the result was divided by 2 to get an approximate value of the apposed surface (AS). ASI was not segmented in a minority of spines whose synapses were oriented obliquely or orthogonally to the cutting plane (5.76% in each stack, across all groups). For each spine the presence of spine apparatus, spinulae in the head or neck of the spine, mitochondria in the presynaptic element, and components of the non-smooth endoplasmic reticulum (tubules, small uncoated vesicles, large coated or uncoated vesicles, multivesicular bodies) was recorded. As previously reported [40, 41] mitochondria were almost always absent inside the spines.

Statistical analysis

Statistical analysis was performed using linear mixed effects (LME) models that include both random and fixed effects. LME models offer several advantages over repeated measures ANOVA including—crucial in our study—the ability to handle unbalanced designs.

The general form of these models is

$$y = Zu + X\beta + \epsilon,$$

where

$$u \sim G(0, \Sigma),$$

and

$$\epsilon \sim G\left(0, \sigma^2 I\right).$$

In these models, y is a vector of response variables (typically log(ASI) values), u is a vector of random effects (mouse and dendrite effects), β is a vector of fixed effects, X and Z are design matrices that link the response variable to the random and fixed effects, and ϵ is a vector of residual values. Both the random effects (u) and the residuals (ϵ) are assumed to have a Gaussian distribution, while the residuals are additionally assumed to be independent with constant variance. Model assumptions of normality and constant variance were assessed and validated graphically using residual plots for all models presented.

Model selection using the Akaike Information Criteria (AIC) was used to identify the set of fixed and random effects in each model. For response variables measured at the dendrite level (synapse density, spine density, diameter), experimental condition was the only fixed effect considered to be included in the models, and mouse was the only random effect considered. For models at the synapse level (ASI, and interactions with the various organelles), we included dendrite as a potential random effect, and synapse density and dendrite diameter as potential fixed effects in the model selection process. In all cases, the AIC selected a model with synapse density, but not dendrite diameter, as a fixed effect and did not include dendrite as a random effect. Maximum likelihood estimates of the parameters in the LME models were calculated numerically using the lmer() function of the lme4 package in R [42], and the statistical significance of effects was assessed using likelihood ratio tests.

LME Model – log(ASI)

The parameter estimates for the fixed effects model of log(ASI), including condition and synapse density as fixed effect are shown in Table 1. The assumption of normally distributed residual values with constant variance was assessed graphically. Based on a scatter plot of the estimated residuals vs. fitted values (Figure 1A), and a quantile-quantile plot of the estimated residuals (Figure 1B), we found no evidence against this assumption.

Scaling analysis

To assess the presence of a scaling relationship, we tested the hypothesis that H_0: $f_1(x) = f_2(x - c)$, i.e. that two probability distributions on a log scale differ only by a location shift. We first estimated c as the difference in the median of the two distributions,

and then transformed the data so that under the null hypothesis they will have the same distribution. Finally, we applied the Kolmogorov-Smirnov test for equality of distribution between two samples. Three potential scaling models were tested to determine the best fit for our data. In the uniform scaling model, every synapse is scaled down by the same amount, while in the selective scaling model a proportion of synapses are randomly selected to be "protected" (not scaled) and the rest are scaled by a fixed amount. In the size-dependent model instead, a proportion of the synapses are randomly selected to be protected, and the likelihood of being protected increases quadratically with synaptic strength (ASI size).

We used a Monte Carlo procedure to estimate the fit of each scaling model. Specifically, a bootstrap procedure was used to generate a random sample of S synapses and a random sample of EW synapses. A scaling model was applied to downscale the EW synapses. The population of scaled-EW synapses was then compared to the population of S synapses. The fit of the model was measured by the Kolmogorov-Smirnov test statistic comparing the distribution of S synapses to the distribution of scaled-EW synapses. This process was repeated 5000 times for each model to estimate its mean squared error (MSE; average KS statistic + variance of KS statistics).

Table 1. Linear mixed effect model for log(ASI)

Random effects	Standard error		
Mouse	0.07472		
Residual	0.89807		
Fixed effects	**Level**	**Estimate**	**Standard error**
Intercept		−2.03871	0.08034
Condition	S (reference)	0	0
	EW	0.29004	0.05951
Synapse Density		−0.31757	0.13984

Results

Two-week-old CD-1 pups spend half of each hour asleep, independent of day or night

We first studied sleep and wake in three pairs of 2-week-old CD-1 siblings housed with the dam (Figure 2A), using behavioral criteria to define each state. This behavioral analysis was necessary because most sleep recordings during early development have been performed in rats or mice in isolation and/or lasted only for a few hours [12, 43]. We specifically avoided the use of electrodes for brain and muscle recordings since a previous study in the rat suggested that they may increase wake time [26]. We also kept the pups with the dam because maternal separation and experimental weaning disrupt normal sleep/wake patterns in neonatal rats [25, 44–46].

Behavior was scored offline in 30-second epochs using behavioral criteria previously established in rats (see Methods for details). Five waking behaviors were distinguished (exploring, grooming, pre-eating/playing, eating, quiet waking) and sleep was defined as any period of immobility lasting more than 15 seconds associated with a decrease in muscle tone. Sleep was further subdivided in quiet sleep and active sleep, the latter characterized by twitching and/or quivering of limbs and/or whiskers. Using these criteria we found that all pups slept approximately half of the 24-hour observation period (47.6 ± 1.4%, mean ± SEM), and total sleep time was almost equally subdivided into active sleep (50.1 ± 2.8%) and quiet sleep (49.9 ± 2.8%; Figure 2B). Consistent with reports in rats [24, 47], time spent in total, active and quiet sleep showed no obvious circadian preference (Figure 2, C and D). Total wake time included eating (25.9 ± 1.5%), grooming (21.9 ± 1.7%), exploratory activity (10.7 ± 0.8%), quiet waking (13.1 ± 0.6%), as well as playing and finding the right nursing position (pre-eating/playing; 28.4 ± 3.7%), Figure 2B). Eating was the only sustained activity observed in the pups, with bouts of nursing often lasting more than 10 minutes.

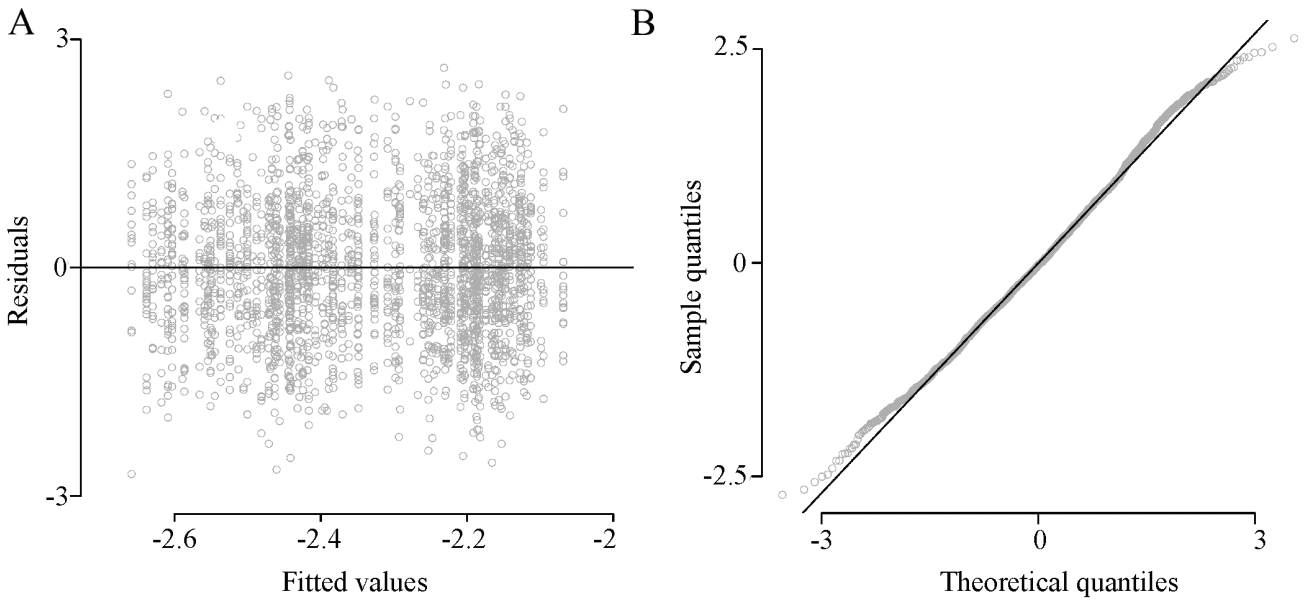

Figure 1. Residual plots. (A) Scatter plot of the estimated residuals vs. the fitted values from the LME model. The plot shows no evidence against the assumption of constant variance for the residuals. (B) Quantile-quantile plot of the estimated residuals to assess normality. A linear relationship between theoretical and sample quantiles suggests a normal distribution for the estimated residuals.

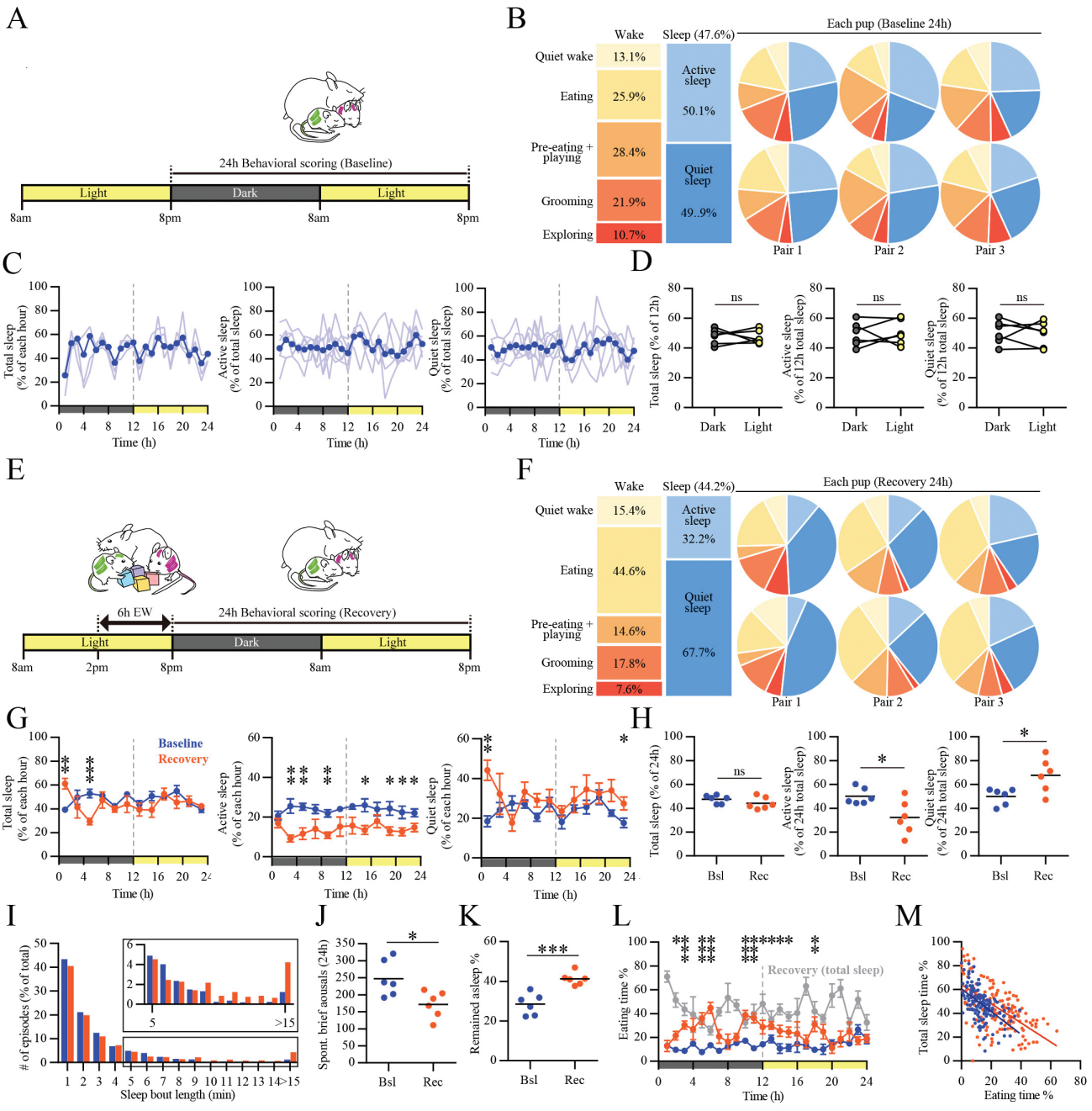

Figure 2. Sleep/wake behavior in 2-week-old CD-1 pups during baseline and after enforced wake. (A) Schematic of the experimental design for 24-hour sleep/wake behavioral analysis during baseline. The two siblings were marked with different colors to be distinguished from each other. (B) Left, average percentage of time spent in wake activities and active or quiet sleep (mean ± SEM, $n = 6$ CD-1 pups). Right, time spent in each behavioral state in each pup. (C) Percentage of each hour spent in total sleep (left), and percentage of active and quiet sleep relative to total sleep for each hour (middle and right). Values are shown for each pup (lighter lines) and averaged across all pups (darker line). (D) Average time spent asleep for each pup during the light and dark periods. (E) Schematic of the experimental design for 6 hours of EW followed by 24 hours of recovery. (F) As in B, for the 24-hour recovery period after EW. (G) Percentage of each hour spent in total, active and quiet sleep for the 24-hour recovery period after EW, plotted in 2-hour bins. The blue line shows the same baseline data as in C, but plotted in 2-hour bins (mean ± SEM, $n = 6$ baseline pups, $n = 6$ recovery pups). Middle panel, AS, post hoc two-tailed independent sample t-test after two-way repeated measures ANOVA, significant difference in hours 3–4 ($t(10) = 4.084$, $p = 0.0022$, Hedge's $g = 2.36$), hours 5–6 ($t(10) = 3.996$, $p = 0.0025$, Hedge's $g = 2.31$), hours 9–10 ($t(10) = 4.585$, $p = 0.0010$, Hedge's $g = 2.65$), hours 15–16 ($t(10) = 3.143$, $p = 0.0105$, Hedge's $g = 1.81$), hours 19–20 ($t(10) = 2.804$, $p = 0.0187$, Hedge's $g = 1.62$), hours 21–22 ($t(10) = 2.69$, $p = 0.0227$, Hedge's $g = 1.55$), hours 23–24 ($t(10) = 2.59$, $p = 0.027$, Hedge's $g = 1.50$. Right panel, QS, post hoc two-tailed t-test after two-way repeated measures ANOVA, significant difference in hours 1–2 ($t(10) = 4.448$, $p = 0.0012$, Hedge's $g = 2.57$) and hours 23–24 ($t(10) = 2.457$, $p = 0.0339$, Hedge's $g = 1.42$). (H) Time spent in total, active and quiet sleep for each pup over the entire 24 hours of baseline and recovery. (I) Distribution of the length of sleep bouts during baseline and recovery (24 hours). (J) Number of spontaneous brief arousals during baseline and recovery (24 hours). (K) Probability that pups remained asleep after being disturbed by their sibling or dam (24 hours). (L) Time spent eating in baseline and after EW (24 hour). As a reference, the gray line shows the time spent asleep in recovery. (M) Negative correlation between time spent eating and sleeping. Each dot represents 1 hour value for one pup. Values are expressed as mean ± SEM. $^{*}p < 0.05$, $^{**}p < 0.01$, $^{***}p < 0.001$; two-tailed independent sample t-test used in (D, H, J, K).

Sleep is homeostatically regulated in 2-week-old CD-1 pups

Next, we asked whether sleep in 2-week-old CD-1 pups is homeostatically regulated, i.e. it changes in duration and/or intensity after a period of sleep deprivation. Three other pairs of siblings were kept awake for 6 hours by gentle handling and by introducing novel objects in their cage (Figure 2E). Pups paid less attention to objects than more mature mice, and were less able to move around the cage to explore. This finding is consistent with the fact that while the sense of smell is functional in newborn rats, hearing and vision mature later, and mouse pups open their eyes only at ~ P13-P14 (refs in [48]). We did not count the number of sleeping attempts, but by the end of the 6 hours pups were trying to fall asleep as soon as they were left undisturbed, suggestive of increased sleep pressure. Their subsequent sleep was compared with sleep in the six pups left undisturbed, which served as controls (Figures 1F and 2B). Total sleep time over the entire 24 hours of recovery did not differ from controls (44.2 ± 2.1% vs. 47.6 ± 1.4% in controls, $t(10) = 1.327$, $p = 0.21$, Hedge's $g = 0.77$; two-tailed t-test) and again showed no circadian preference (Figure 2G). However, a significant sleep rebound was present in the first 2 hours of recovery, when time spent asleep increased to 61.2 ± 4.5% as compared to 39.2 ± 2.4% in controls (Figure 2G, left; two-way repeated measures ANOVA, significant interaction between Mouse group and Time ($F(11,110) = 3.16$, $p = 0.0010$, followed by post hoc two-tailed t-test; $t(10) = 4.307$, $p = 0.0015$, Hedge's $g = 2.49$). This early sleep rebound was followed by a significant decrease in hours 5–6 (Figure 2G, left; 29.3 ± 2.8% vs. 52.8 ± 3.7% in controls; $t(10) = 5.064$, $p = 0.0005$, Hedge's $g = 2.9$; two-tailed t-test) due to a sustained increase in time spent eating (Figure 2L; 40.4 ± 2.9% vs. 10.6 ± 2.0% in controls; two-way repeated measures ANOVA, significant interaction between Mouse group and Time ($F(23,230) = 3.362$, $p < 0.0001$), followed by post hoc two-tailed t-test; $t(10) = 8.532$, $p = 0.000007$, Hedge's $g = 4.93$; two-tailed t-test). As compared to controls, during the entire recovery period pups spent consistently less time in active sleep, while time spent in quiet sleep increased only at the beginning and at the end of the recovery period (Figure 2G, middle, right; two-way repeated measures ANOVA; AS, significant effect of Mouse group ($F(1,10) = 14.42$, $p = 0.0035$; QS, significant interaction between Mouse group and Time ($F(11,110) = 2.742$, $p = 0.0036$). In all pups most sleep episodes were short (<5 minutes), but after sleep loss the longer bouts were more frequent and average bout length increased relative to controls (4.9 ± 0.2 vs. 7.3 ± 0.9 minutes in recovery; $t(10) = 2.584$, $p = 0.0272$, Hedge's $g = 1.49$; Figure 2I). When we computed the total amount of sleep for each pup we also distinguished between "disturbed" and "undisturbed" sleep, scoring a sleep epoch as disturbed if the sleeping pup was nudged by the sibling or the dam, and recording whether this brief disturbance resulted in a brief arousal. If it did, we called this an "evoked awakening" to distinguish it from spontaneous brief arousals. After enforced wake the number of spontaneous brief arousals decreased (171.8 ± 16.0 vs. 247.7 ± 21.5 in controls; $t(10) = 2.829$, $p = 0.0179$, Hedge's $g = 1.63$; Figure 2J) and so did the number of evoked awakenings (280.7 ± 23.6 vs. 348.2 ± 10.4 in controls, $t(10) = 2.619$, $p = 0.0256$, Hedge's $g = 1.51$). In other words, the probability to remain asleep after being disturbed increased after enforced wake (41.3 ± 1.3% vs. 28.5 ± 2.2% in controls; $t(10) = 4.969$, $p = 0.00056$, Hedge's $g = 2.87$; Figure 2K), despite the fact that disturbed sleep as percentage of total sleep did not differ between baseline and recovery groups (disturbed: baseline 37.3 ± 2.4% of total sleep time vs. 38.5 ± 2.1% after EW; $t(10) = 0.3857$, $p = 0.7078$, Hedge's $g = 0.22$). Together, the decline in both spontaneous and evoked awakenings is consistent with deeper sleep. Finally, during enforced wake pups struggled to eat, because soon after assuming the nursing position they would fall asleep and had to be awakened. During recovery pups spent more time eating (44.1 ± 3.8% of total wake time vs. 25.9 ± 1.5% in controls, $p = 0.00134$; Figure 2, B and F). In fact, after enforced wake pups switched mainly between two activities, eating and sleeping (Figure 2, L and M).

Two-week-old YFP-H pups are asleep half of each hour during the day and sleep longer after sleep deprivation

We then focused on the YFP-H mouse strain that was used to characterize synaptic changes in adolescent (P30) mice [11] and in three pairs of siblings we performed a behavioral analysis similar to the one done in the CD-1 strain. Due to their dark fur and small size YFP-H pups could be reliably scored only during the day and we did not attempt to distinguish between active and quiet sleep (see Methods for details). Despite these limitations, we could confirm the two major findings obtained in CD-1 pups (Figure 3A): (1) during the light phase P13 pups spent roughly 50% of each hour asleep; (2) 4–4.5 hours of sleep deprivation starting at light onset led to an immediate rebound in sleep duration in the first 2 hours of recovery.

In a different experiment other P13 YFP-H pups were used to assess the effects of acute sleep deprivation on body weight. After 4–8 hours of extended wake body weight decreased to ~96% of the value measured at light onset just before the beginning of the experiment ($n = 10$ pups; % weight relative to light onset; mean ± SD, 4-hour EW = 97.47 ± 1.34; 8-hour EW = 94.53 ± 1.27).

In 2-week-old YFP-H pups sleep is associated with a decrease in the size of the ASI

Next, we used SBEM to determine whether in YFP-H P13 pups cortical synapses differ in size between wake and sleep. In the previous study in adolescent (P30) mice [11] we focused on layer 2 of primary motor cortex and primary sensory cortex because there is compelling evidence for activity-dependent structural plasticity in these areas and layers [10]. We measured the ASI, the area of contact between spine head and presynaptic terminal or bouton, which is an established ultrastructural measure of synaptic strength, as well as the volume of the spine head, which is positively correlated with the ASI [49–51], and compared mice after spontaneous sleep, spontaneous wake at night, and forced wake during the day. We found consistent results across cortical areas using both structural measures, and found similar differences in both wake conditions relative to sleep. Here we did not try to collect two wake groups, because 2-week-old CD-1 pups were never spontaneously awake for several hours at night. Thus, all brains were collected in the middle of the light phase, after pups were either allowed to sleep ad libitum for 4.5 to 6 hours (S group) or kept awake as much as possible for the same period of time (enforced wake, EW group, Figure 3B; 5 mice/group, see Methods). Like CD-1 pups, YFP-H pups were weakly responsive

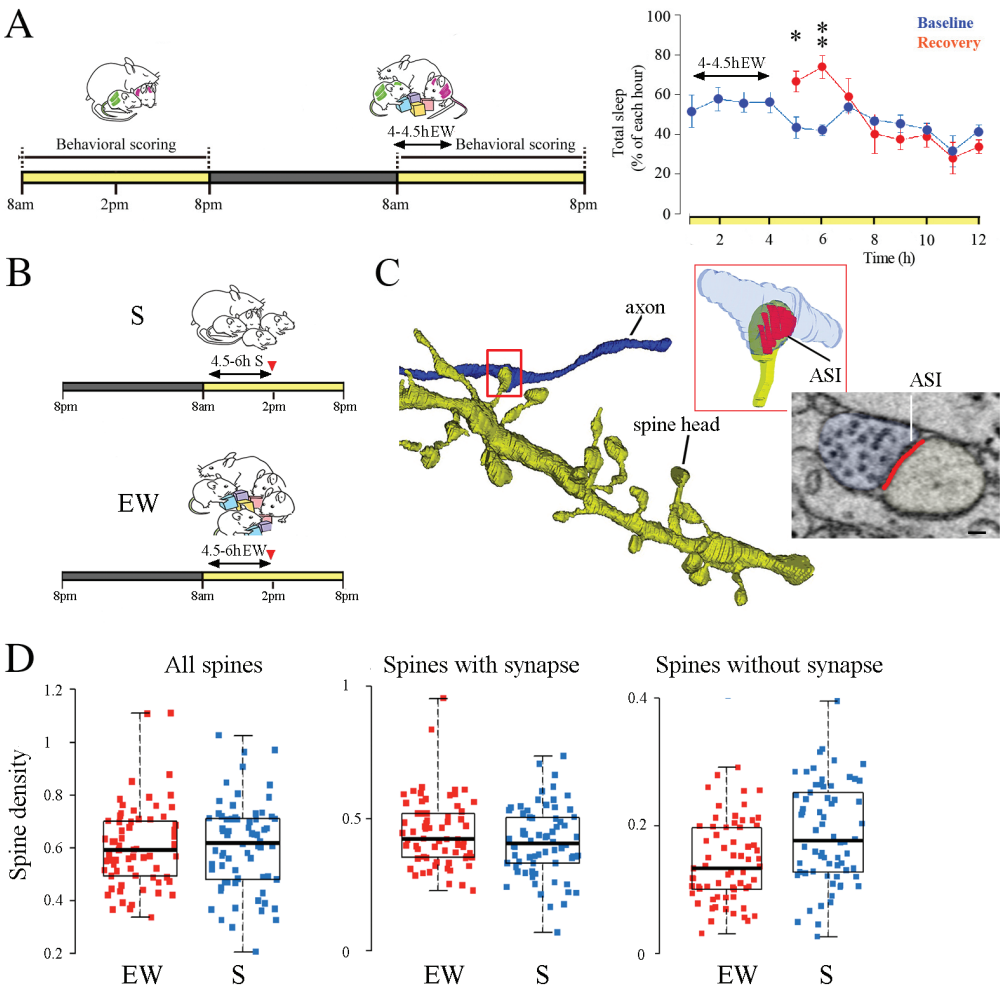

Figure 3. Diffuse downscaling of synapses after sleep relative to enforced wake in YFP-H pups. (A) Left, schematic of the experimental design for sleep/wake scoring in B6.Cg-Tg(Thy1-YFP)16Jrs/J (YFP-H) mice during the light period (P13) followed the next day by 4–4.5 hours of EW. Right, percentage of each hour spent in total sleep during the baseline light period and after 4–4.5 hours EW, plotted in 1-hour bins (mean ± SEM, $n = 6$ YFP-H pups). Two-tailed paired sample t-test, $^{*}p < 0.05$, $^{**}p < 0.01$; significant differences in hour 5 ($t(5) = 3.8599$, $p = 0.0119$, Cohen's $d = 1.58$) and hour 6 ($t(5) = 4.504$, $p = 0.0064$, Cohen's $d = 1.84$). (B) Schematic of the experimental design for the ultrastructural studies. Red arrowheads indicate time of brain collection. (C) Example of one of the dendritic segments reconstructed in this study (all segments are shown in Figure 4). The contact between the axon and a single spine head (red box) is shown in greater detail in the top right corner, with the ASI in red. Bottom right, raw image of a synapse with ASI in red. Scale bar = 100 nm. (D) Effect of condition on spine density (N of spines/μm²) for all dendritic segments. Each dot represents one dendritic segment. (E) Effect of condition on ASI size. ASI size is shown for all synapses, each represented by one dot. (F) Estimated probability densities reveal a log-normal distribution of ASI size (main panel: μm², inset: log transformed) in the two experimental groups. (G) Scaling of ASI between wake and sleep. (H) Monte Carlo simulations comparing different scaling models parametrized by the proportion of synapses that undergo scaling. The x-axis corresponds to the proportion of synapses that scale in the model and the y-axis corresponds to the mean squared error of the model (lower values indicate better model fit). Size-dependent (green) and selective scaling independent of size (brown) do not outperform uniform scaling (asterisk).

to novel objects, and it is very likely that short periods of sleep did occur during EW. As in the previous study blocks of cortical tissue (~25 by 25 by 20 μm) were automatically aligned and spiny dendritic segments were manually segmented by trained annotators (Figures 3C and 4). Dendrites were randomly selected within each block and balanced in size between groups (no effect of condition on diameter, $p = 0.2722$; diameter = 0.68 ± 0.10 μm, mean ± SD, Table 2), for a total of 136 dendritic segments (10–18 dendrites/mouse; Figure 4). All protrusions (spines) were annotated, including spines forming synapses and spines without synapses (27.3% of all protrusions; Table 2).

To characterize the effect of sleep and wake on number and size of synapses we used a LME model that included mouse as a random effect and condition (S, EW) as categorical fixed effect (see Methods, LME models). Condition had no effect on total spine density ($p = 0.95$) or synapse density ($p = 0.20$), while a trend was present for more spines lacking synapses after sleep ($p = 0.094$; Figure 3D). For the ASI analysis we included dendrite as an additional random effect in the model, and synapse density (number of synapses by surface area) as an additional linear fixed effect. Condition had instead a large effect on ASI ($\chi^2 = 12.21$, df = 1, $p = 0.0005$; Figure 3E), which did not interact with synapse density ($p = 0.3292$). On average, ASI sizes after sleep were reduced by 33.9% relative to enforced wake.

At the population level, all synapses are equally likely to downscale with sleep

As in P30 mice, ASI size followed a log-normal distribution, with many small synapses and a few large ones. Moreover, the distribution of ASI size in the S group was shifted to the left relative to the EW group (Figure 3F), suggesting that synapses shrank

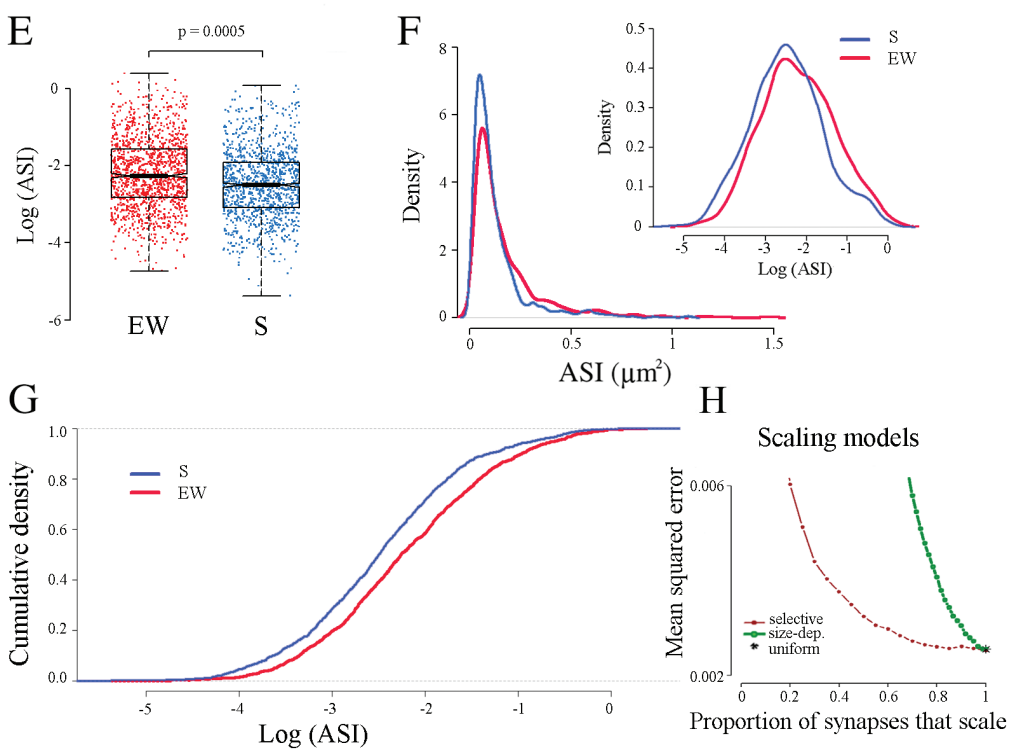

Figure 3. Continued

Table 2. Summary of ultrastructural measures

Experimental condition	EW	S
Total N of dendrites = 136	66	70
Total N of spines (with/without synapses) = 3750	1923	1827
Total N of spines with synapse = 2722	1459	1263
Total N of spines without synapse = 1028	464	564
Total N of spines with measured ASI (oblique and incomplete excluded) = 2506	1333	1173
ASI (μm², mean ± SD) range (μm²)	0.168 ± 0.177 (0.009, 1.481)	0.127 ± 0.141 (0.005, 1.082)
Spine density (all protrusions) (#/μm², mean ± SD)	0.615 ± 0.161	0.617 ± 0.176
Density of spines with synapse (#/μm², mean ± SD)	0.471 ± 0.138	0.431 ± 0.145
Density of spines without synapse (#/μm², mean ± SD)	0.144 ± 0.064	0.187 ± 0.078
Oblique spines (% per mouse of complete spines with synapse)	6.79 ± 1.54%	4.39 ± 2.02%
Incomplete spines (% per mouse of spines that go off the image)	3.13 ± 1.64%	3.21 ± 2.72%
Spines without synapse (% per mouse)	23.88 ± 2.47%	30.46 ± 6.42%
Dendrite diameter (μm, mean ± SD)	0.689 ± 0.095	0.668 ± 0.111
Dendrite length (μm, mean ± SD)	22.998 ± 7.232	20.529 ± 6.589
Spines with spine apparatus (% per mouse, mean ± SD)	10.19 ± 3.19%	8.89 ± 4.65%
Spines with non-SER elements (tubules/vesicles/MVBs; % per mouse, mean ± SD)	72.05 ± 7.06%	68.44 ± 4.56%
Synapses with mitochondrion in the axonal bouton (% per mouse, mean ± SD)	24.91 ± 2.22%	25.86 ± 3.95%
Synapses with mitochondrion in the shaft (% per mouse, mean ± SD)	92.61 ± 4.02%	90.06 ± 6.48%
Spines with coated vesicles in the head/neck (% per mouse, mean ± SD)	9.74 ± 2.49%	8.38 ± 3.59%
Spines with a spinula (% per mouse, mean ± SD)	1.25 ± 1.13%	1.99 ± 2.29%
Spines with a MVB in head/neck/base (% per mouse, mean ± SD)	11.86 ± 2.74%	10.70 ± 3.11%
Branched spines (% per mouse, mean ± SD)	18.58 ± 2.64%	15.95 ± 2.86%

All protrusions are defined as spines. In oblique spines the ASI could not be measured because the synapse was oriented obliquely or orthogonally to the cutting plane. Non-SER = components of the non-smooth endoplasmic reticulum. MVB, multivesicular bodies. EW, enforced wake group. S, sleep group. B6.Cg-Tg(Thy1-YFP)16Jrs/J mice were used (YFP-H mice).

with sleep in a manner proportional to their size (scaling). Formal testing found no evidence against a scaling relationship between S and EW synapses ($p = 0.2388$; Figure 3G). In other words, the differences between conditions were consistent with multiplicative scaling (or a location shift on the log scale) by an estimated scaling factor of 0.786, i.e. S synapses were scaled down to 78.6% of the size of EW synapses. We then performed Monte Carlo simulations on bootstrapped data (Methods) to test which type of scaling best accounted for the results. Size-independent selective scaling and size-dependent scaling did

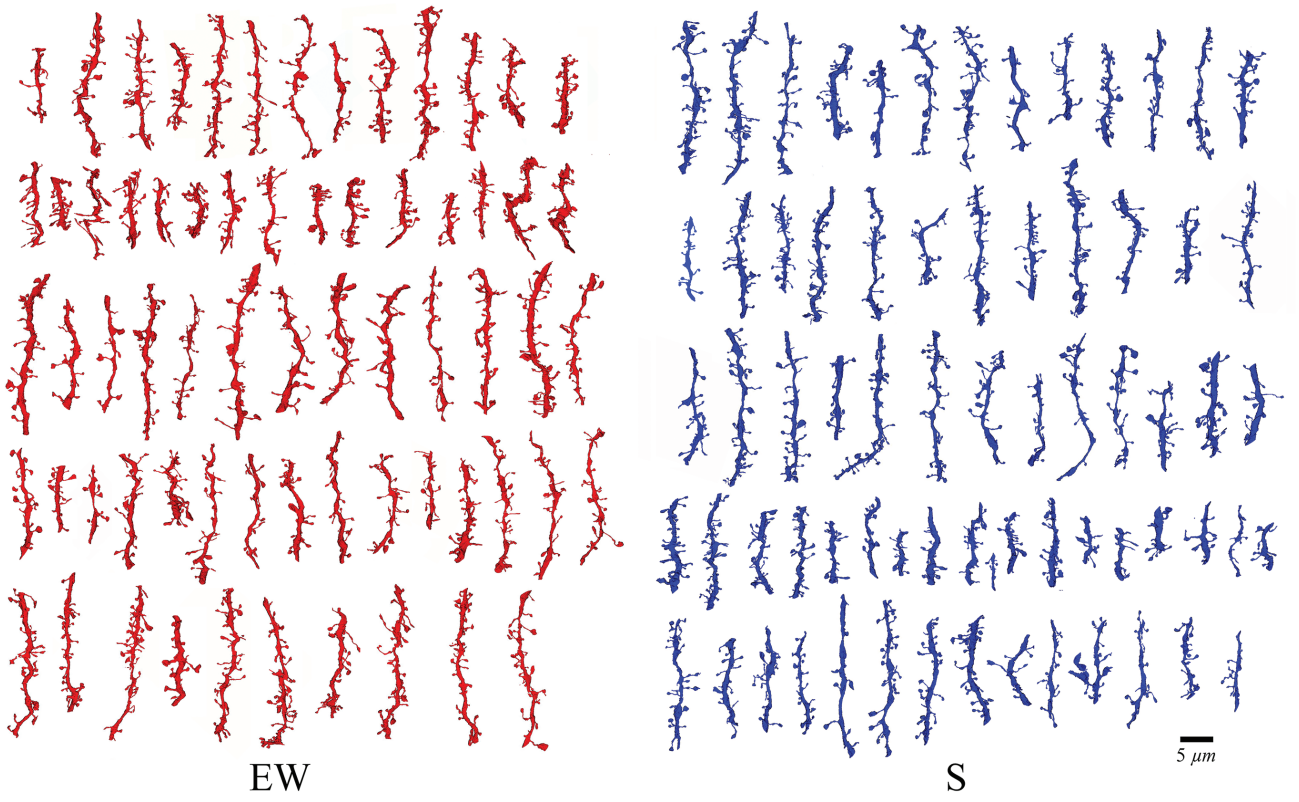

Figure 4. Reconstruction of all dendritic segments used in the study. EW, enforced wake group. S, sleep group. Within each group, all dendritic segments from one individual animal are shown in a single row.

not outperform uniform scaling (Figure 3H), suggesting that all synapses, independent of their size, were equally likely to downscale with sleep.

Finally, we tested whether specific features of the spine morphology predicted the likelihood to undergo sleep/wake changes. We found no interaction between condition and spine shape (stubby or not), presence of endosomes, spine apparatus or spinula in the spine, and presence of one or more mitochondria in the axonal bouton facing the spine (Figure 5).

Discussion

In this study we describe the sleep/wake pattern and the response to extended wake in pre-weaned mouse pups of two strains recorded in conditions as physiological as possible, i.e. keeping the siblings with the dam and avoiding invasive methods to identify behavioral states. Our behavioral analysis was first performed in CD-1 mice because their white fur made behavioral scoring possible under red light conditions at night. The major findings obtained in CD-1 mice were then confirmed in the YFP-H strain that was used for the ultrastructural experiments, to allow direct comparison of the results of the current study with those obtained in P30 mice [11]. We found that 2-week-old CD-1 pups spend roughly half of each of the 24 hours asleep and show a clear homeostatic response to a few hours of enforced wake, including an immediate increase in total sleep duration and a sustained increase in quiet sleep at the expense of active sleep. Enforced wake at this age also leads to deeper and more consolidated sleep, characterized by fewer brief arousals, longer sleep bouts, and a decreased propensity to awaken in response to natural stimuli. These latter findings are consistent with the early expression of sleep pressure and sleep rebound described in 1- to 2-week-old rats [52, 53]. During the light phase YFP-H pups also spend half of each hour asleep and sleep longer immediately after sleep deprivation, although we cannot rule out that their night sleep pattern may have differed from the pattern that we report in CD-1 pups.

To the best of our knowledge this behavioral analysis had not been previously done in mice. We studied 2-week-old pups because at this age the rodent brain is still undergoing significant developmental changes but sleep and wake can be identified using behavioral criteria (reviewed in [52]). In rats, the cerebral cortex undergoes an explosive expansion between postnatal day 0 (P0), when the brain is only 15% of its final size, and P10, when cells and especially axons and dendrites have completed most of their growth [12]. During this early postnatal period, when a close association between behavioral states and cortical EEG patterns has yet to be established, cortical activity is dominated by spindle bursts, often triggered from the periphery and relayed to the cortex via thalamic inputs. By the end of the second postnatal week many cortico-cortical synapses are formed, total EEG power increases, and EEG patterns become continuous due to the appearance of sleep slow waves [12, 43, 54]. Studies in rats pointed to around P12 as the earliest time when, due to the prominence of slow waves, behaviorally defined quiet sleep can be distinguished at the EEG level from wake and active sleep [26, 27, 55, 56]. This finding was confirmed in two strains of mice [29] and more recent work in rats found that by P14 slow wave activity is only associated with quiet sleep [57, 58]. In mouse pups longitudinal video-EEG recordings (P9–P21) performed daily for 3

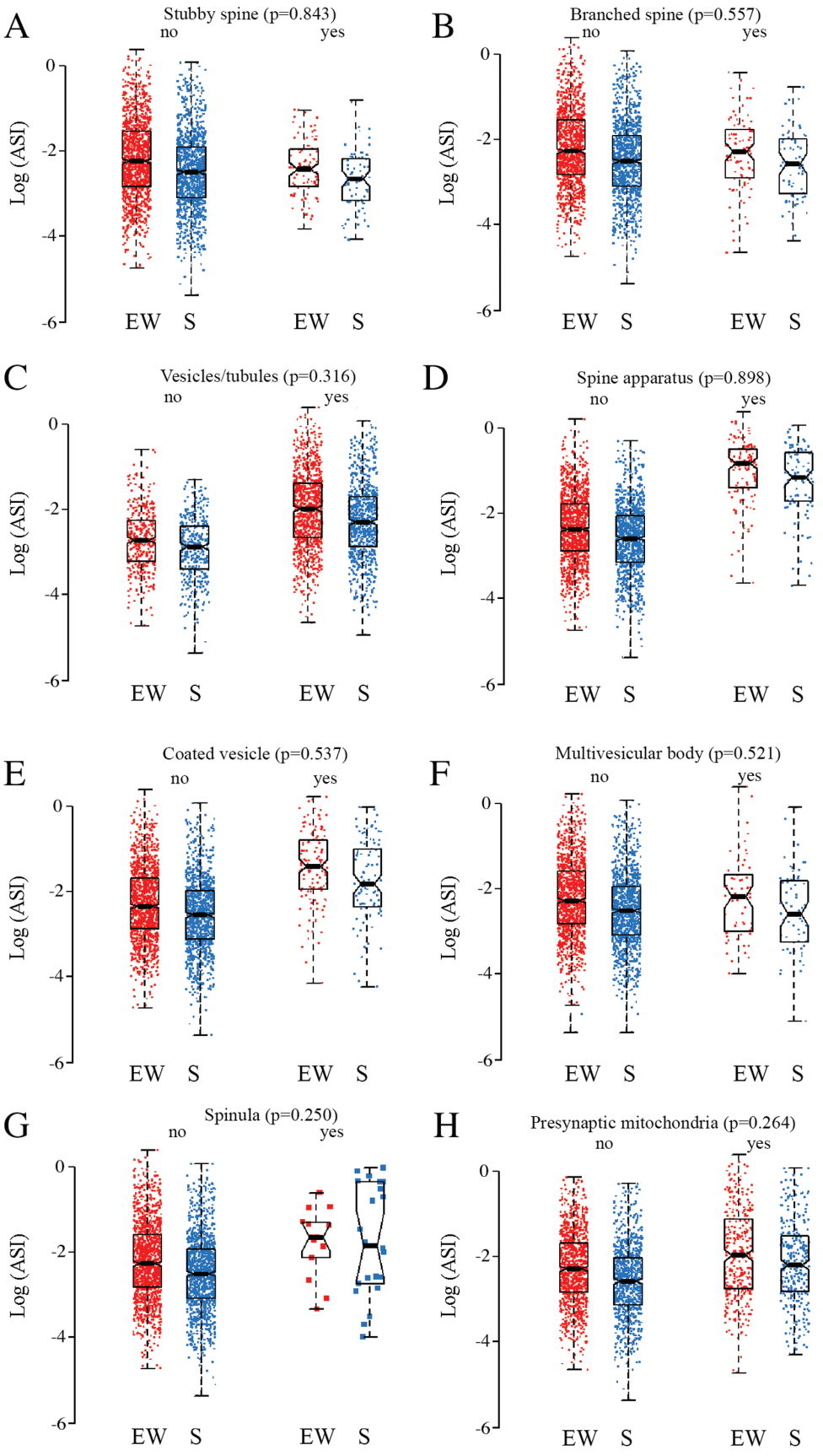

Figure 5. Lack of significant effect of condition (EW, S) on spine morphological features. EW, enforced wake group. S, sleep group. ASI size is shown for all synapses, each represented by one dot. "No" and "yes" refer to the absence or presence of each morphological feature, respectively.

hours during the light phase found evidence for sleep/wake specific EEG patterns as early as P10, and complete disappearance of EEG discontinuity by P14 [43]. In most of these experiments pups were studied in isolation, for only 1–3 hours to avoid the confounding effect of hunger, and/or using invasive methods. Overall, in these reports 2-week-old animals were awake 20%–40% of the total recorded time, less than the ~50% we found. Rats recorded continuously for 24 hours at P12 and P14 were also found to be awake ~20% of time; in that study pups were separated from the dam and prefitted with cheek cannulas to be fed every 35 minutes via a feeding tube [59]. Thus, the higher percent of time spent awake in our study relative to the previous reports may be explained by our finding that time spent eating, or preparing to eat, accounts for a large fraction of the 24-hour cycle when pups are kept with the dam; eating-related wake activities are instead underestimated when pups are separated from the dam and/or artificially fed. Independent of the merit of this explanation, we note that the two main conclusions of our behavioral analysis remain valid: 2-week-old pups show signs of homeostatic sleep regulation in response to a few hours of sleep loss, and are unable to spontaneously stay awake for several hours. These behavioral findings justify the use of only two experimental groups (S, EW) for the ultrastructural experiments.

In CD-1 pups we also found that time spent asleep was equally divided between active and quiet sleep. A recent study in rats found similar results when the authors did not rely on the EEG to score behavioral states, but higher values of quiet sleep when they did [58]. A recent EEG study in mouse pups (P12–P14) also reports higher values of quiet sleep than of active sleep [43]. Thus, our behavioral observations most likely underestimated the time spent in quiet sleep. Due to their small size we did not try to distinguish active from quiet sleep in YFP-H pups. As in our previous studies [4, 11], however, the goal of the ultrastructural experiments was to compare the synaptic effects of wake to those of total sleep, independent of the exact percentage of time spent in quiet and active sleep.

The main goal of this study was to test whether the need for sleep-dependent synaptic renormalization also applies to the immature brain that is still growing. Direct evidence for or against this idea was lacking. It was suggested that an immature brain may either not need this renormalization [21] or require it even more than the adult brain [3, 22]. We found that in pre-weaned pups synapses in layer 2 of primary motor cortex have a smaller ASI after a period of sleep than after a sustained period of wake. Because ASI, post-synaptic density and spine volume are positively correlated [51, 60, 61], these results suggest that synapses may also be smaller after sleep than after wake. Moreover, because ASI and post-synaptic density are correlated with the synaptic expression of glutamatergic AMPA receptors and with the strength of excitatory synaptic currents [62–64], these results suggest that synapses in layer 2 of primary motor cortex are weaker after sleep as compared to after wake. The observed changes could be described as a global sleep-dependent downscaling, at least at the population level. Scaling signifies that the changes are not additive but proportional to synapse size (multiplicative) and global indicates that all spines are likely to change across the sleep/wake cycle, independent of their size and of the presence of specific spine organelles. Note, however, that these conclusions are based on statistical analyses performed at the population level, since we could not follow individual synapses across the sleep/wake cycle. Thus, we do not know whether changes are necessarily multiplicative at the level of each single synapse. It is known, however, that learning during wake requires selective changes in synaptic efficacy, rather than homogeneous scaling (e.g. [65, 66]). Thus, although we cannot provide direct evidence, it is unlikely that the sleep/wake differences that we report are solely driven by global upscaling during wake.

YFP-H pups reached ~96% of their initial body weight after 4 to 8 hours of extended wake. This weight loss is comparable or smaller than the one recently reported after 3 hours of EEG recordings in pups kept in isolation [43] and occurred despite the presence of the dam, underscoring the difficulty in maintaining a regular feeding schedule when pups are repeatedly stimulated to prevent their sleep. This weight loss, however, is unlikely to account for the increase in ASI size observed after extended wake because the growth of synapses requires energy and decreased food intake is expected to decrease, rather than increase, ASI size. Indeed starving (16–48 hours) in adult mice inhibits cell growth, increases autophagy in the liver and brain, including the cerebral cortex, and inhibits the mTOR pathway that mediates the dendritic synthesis of proteins required for long-term changes in synaptic strength [67]. Moreover, the change in ASI size observed in pre-weaned pups is in the same direction described in more mature, post-weaned, mice that could feed ad libitum. The mechanisms underlying the synaptic changes described here remain unknown. Catecholamines and glucocorticoids promote optimal performance and synaptic plasticity and future experiments should determine whether their levels increased in young pups kept awake and if so, whether they contributed to the sleep/wake changes in synaptic strength.

In layer 2 of primary motor cortex the difference in ASI size between sustained wake and sleep was on average larger in pups than in adolescent mice (~34% vs. 18% at P30) and occurred across all synapses, while at P30 spines were less likely to change if they were large and if they lacked endosomes and vesicles of the non-smooth endoplasmic reticulum [11]. We speculate that P13 synapses, even when large, may still be not fully committed and thus are less protected from downscaling. Consistent with this hypothesis, even the larger synapses in pups were substantially smaller than those in P30 adolescent mice (ASI in μm^2, mean ± SD and range: P13 S mice = 0.127 ± 0.141, 0.005–1.082; P13 EW mice = 0.168 ± 0.177; 0.009–1.481; Table 2; P30 S mice = 0.256 ± 0.289, 0.010–2.038; P30 EW mice = 0.294 ± 0.324, 0.007–3.543 [11]). Whether these results apply to other cortical regions and layers is unknown. Previous studies showed that during the first postnatal week there is greater and more complex spontaneous activity in primary sensory cortex than in primary motor cortex [68]. Thus, although in P30 adolescent mice changes in primary motor and sensory cortex were similar, we cannot assume that this is also the case in pups.

In summary, our results suggest that sleep-dependent synaptic renormalization occurs on a broad scale in layer 2 of the pre-weaned primary motor cortex, at a crucial time for the development and refinement of neural circuits [12]. Whether these findings extend to even earlier developmental times remains to be investigated, not least because assessing and preventing sleep in very young animals is challenging [14]. It is possible that during the early, experience-independent phase of synaptic formation and refinement [69] spontaneous activity during sleep might serve to restore synaptic homeostasis also in the positive direction, to avoid the risk that a neuron may form too few

connections [22]. In *Drosophila*, protracted sleep deprivation immediately after eclosion impairs the development of the fastest growing olfactory glomerulus, but not of the other glomeruli [18]. Thus, future experiments should also examine, in addition to the potential positive effects of sleep on synaptic renormalization, the potential negative effects of early sleep deprivation on synaptogenesis.

Supplementary material

Supplementary material is available at *SLEEP* online.
Video 1. Example of active sleep.
Video 2. Example of quiet sleep.

Funding

Supported by grants National Institutes of Health (NIH) Director's Pioneer Award DP 1OD579 (G.T.), NIH/NIMH grant 1R01MH091326 (G.T.), NIH/NIMH grant 1R01MH099231 (G.T., C.C.), and NIH/NINDS grant 1P01NS083514 (G.T., C.C.) and Japan Society for the Promotion of Science (JSPS) Overseas Research Fellowships H26-202 (H.N.).

Acknowledgments

We thank Kort A. Driessen for help in the behavioral analysis. *Author contributions*: L.dV., H.N., N.dW., G.M.S., M.B. collected and analyzed data; W.M., K.M.N., S.S.S., M.N. analyzed data; L.dV., H.N., G.T., C.C. designed the experiments; L.dV., H.N., N.dW., G.M.S., W.M., G.T., and C.C. wrote the article.
Conflict of interest statement. None declared.

References

1. Cirelli C. Sleep, synaptic homeostasis and neuronal firing rates. *Curr Opin Neurobiol*. 2017;**44**:72–79.
2. Tononi G, Cirelli C. Sleep and synaptic down-selection. *Eur J Neurosci*. 2019. doi:10.1111/ejn.14335. [Epub ahead of print] Review.
3. Tononi G, *et al*. Sleep and the price of plasticity: from synaptic and cellular homeostasis to memory consolidation and integration. *Neuron*. 2014;**81**(1):12–34.
4. Vyazovskiy VV, *et al*. Molecular and electrophysiological evidence for net synaptic potentiation in wake and depression in sleep. *Nat Neurosci*. 2008;**11**(2):200–208.
5. Huber R, *et al*. Human cortical excitability increases with time awake. *Cereb Cortex*. 2013;**23**(2):1–7.
6. Gulati T, *et al*. Neural reactivations during sleep determine network credit assignment. *Nat Neurosci*. 2017;**20**(9):1277–1284.
7. Norimoto H, *et al*. Hippocampal ripples down-regulate synapses. *Science*. 2018;**359**(6383):1524–1527.
8. Diering GH, *et al*. Homer1a drives homeostatic scaling-down of excitatory synapses during sleep. *Science*. 2017;**355**(6324):511–515.
9. Bartram J, *et al*. Cortical Up states induce the selective weakening of subthreshold synaptic inputs. *Nat Commun*. 2017;**8**(1):665.
10. Holtmaat A, *et al*. Experience-dependent structural synaptic plasticity in the mammalian brain. *Nat Rev Neurosci*. 2009;**10**(9):647–658.
11. de Vivo L, *et al*. Ultrastructural evidence for synaptic scaling across the wake/sleep cycle. *Science*. 2017;**355**(6324):507–510.
12. Cirelli C, *et al*. Cortical development, electroencephalogram rhythms, and the sleep/wake cycle. *Biol Psychiatry*. 2015;**77**(12):1071–1078.
13. Del Rio-Bermudez C, *et al*. Active Sleep Promotes Functional Connectivity in Developing Sensorimotor Networks. *Bioessays*. 2018;**40**(4):e1700234.
14. Frank MG. Sleep and developmental plasticity not just for kids. *Prog Brain Res*. 2011;**193**:221–232.
15. Marks GA, *et al*. A functional role for REM sleep in brain maturation. *Behav Brain Res*. 1995;**69**(1-2):1–11.
16. Mirmiran M. The function of fetal/neonatal rapid eye movement sleep. *Behav Brain Res*. 1995;**69**(1-2):13–22.
17. Dumoulin Bridi MC, *et al*. Rapid eye movement sleep promotes cortical plasticity in the developing brain. *Sci Adv*. 2015;**1**(6):e1500105.
18. Kayser MS, *et al*. A critical period of sleep for development of courtship circuitry and behavior in Drosophila. *Science*. 2014;**344**(6181):269–274.
19. Kayser MS, *et al*. Sleep and development in genetically tractable model organisms. *Genetics*. 2016;**203**(1):21–33.
20. Seugnet L, *et al*. Sleep deprivation during early-adult development results in long-lasting learning deficits in adult Drosophila. *Sleep*. 2011;**34**(2):137–146.
21. Frank MG. Erasing synapses in sleep: is it time to be SHY? *Neural Plast*. 2012;**2012**:264378.
22. Tononi G, *et al*. Time to be SHY? Some comments on sleep and synaptic homeostasis. *Neural Plast*. 2012;**2012**:415250.
23. *Guide for the Care and Use of Laboratory Animals: Eighth Edition*. Washington: The National Academies Press; 2011:1–220.
24. Bolles RC, *et al*. The ontogeny of behaviour in the albino rat. *Animal Behaviour*. 1964;**12**:427–441
25. Jouvet-Mounier D, *et al*. Ontogenesis of the states of sleep in rat, cat, and guinea pig during the first postnatal month. *Dev Psychobiol*. 1970;**2**(4):216–239.
26. Hilakivi LA, *et al*. Sleep-wake behavior of newborn rats recorded with movement sensitive method. *Behav Brain Res*. 1986;**19**(3):241–248.
27. Gramsbergen A, *et al*. The postnatal development of behavioral states in the rat. *Dev Psychobiol*. 1970;**3**(4):267–280.
28. Blumberg MS, *et al*. A developmental and component analysis of active sleep. *Dev Psychobiol*. 1996;**29**(1):1–22.
29. Daszuta A, *et al*. Early postnatal development of EEG and sleep-waking cycle in two inbred mouse strains. *Brain Res*. 1985;**354**(1):39–47.
30. Franken P, *et al*. Sleep deprivation in rats: effects on EEG power spectra, vigilance states, and cortical temperature. *Am J Physiol*. 1991;**261**(1 Pt 2):R198–R208.
31. Bellesi M, *et al*. Sleep and wake affect glycogen content and turnover at perisynaptic astrocytic processes. *Front Cell Neurosci*. 2018;**12**:308.
32. Bellesi M, *et al*. Myelin modifications after chronic sleep loss in adolescent mice. *Sleep*. 2018;**41**(5). doi:10.1093/sleep/zsy034.
33. Nelson AB, *et al*. Sleep patterns and homeostatic mechanisms in adolescent mice. *Brain Sci*. 2013;**3**(1):318–343.
34. Schindelin J, *et al*. Fiji: an open-source platform for biological-image analysis. *Nat Methods*. 2012;**9**(7):676–682.
35. Fiala JC, *et al*. Cylindrical diameters method for calibrating section thickness in serial electron microscopy. *J Microsc*. 2001;**202**(Pt 3):468–472.
36. Cardona A, *et al*. TrakEM2 software for neural circuit reconstruction. *PLoS One*. 2012;**7**(6):e38011.

37. van Aerde KI, *et al*. Morphological and physiological characterization of pyramidal neuron subtypes in rat medial prefrontal cortex. *Cereb Cortex*. 2015;**25**(3):788–805.
38. Larkman AU. Dendritic morphology of pyramidal neurones of the visual cortex of the rat: I. Branching patterns. *J Comp Neurol*. 1991;**306**(2):307–319.
39. Kawaguchi Y, *et al*. Dendritic branch typing and spine expression patterns in cortical nonpyramidal cells. *Cereb Cortex*. 2006;**16**(5):696–711.
40. Knott GW, *et al*. Spine growth precedes synapse formation in the adult neocortex in vivo. *Nat Neurosci*. 2006;**9**(9):1117–1124.
41. Kasthuri N, *et al*. Saturated Reconstruction of a Volume of Neocortex. *Cell*. 2015;**162**(3):648–661.
42. Bates D, *et al*. Fitting linear mixed-effects models using lme4. *J Stat Softw*. 2015;**67**:1–48.
43. Rensing N, *et al*. Longitudinal analysis of developmental changes in electroencephalography patterns and sleep-wake states of the neonatal mouse. *PLoS One*. 2018;**13**(11):e0207031.
44. Hofer MA, *et al*. Control of sleep-wake states in the infant rat by features of the mother-infant relationship. *Dev Psychobiol*. 1982;**15**(3):229–243.
45. Hofer MA. The organization of sleep and wakefulness after maternal separation in young rats. *Dev Psychobiol*. 1976;**9**(2):189–205.
46. Suchecki D, *et al*. Maternal regulation of the hypothalamic-pituitary-adrenal axis in the infant rat: the roles of feeding and stroking. *Brain Res Dev Brain Res*. 1993;**75**(2):185–192.
47. Frank MG, *et al*. Development of diurnal organization of EEG slow-wave activity and slow-wave sleep in the rat. *Am J Physiol*. 1997;**273**(2 Pt 2):R472–R478.
48. Alberini CM, *et al*. Infantile amnesia: a critical period of learning to learn and remember. *J Neurosci*. 2017;**37**(24):5783–5795.
49. Desmond NL, *et al*. Synaptic interface surface area increases with long-term potentiation in the hippocampal dentate gyrus. *Brain Res*. 1988;**453**(1-2):308–314.
50. Buchs PA, *et al*. Induction of long-term potentiation is associated with major ultrastructural changes of activated synapses. *Proc Natl Acad Sci U S A*. 1996;**93**(15):8040–8045.
51. Cheetham CE, *et al*. Pansynaptic enlargement at adult cortical connections strengthened by experience. *Cereb Cortex*. 2014;**24**(2):521–531.
52. Todd WD, *et al*. Brainstem and hypothalamic regulation of sleep pressure and rebound in newborn rats. *Behav Neurosci*. 2010;**124**(1):69–78.
53. Frank MG, *et al*. Effects of sleep deprivation in neonatal rats. *Am J Physiol*. 1998;**275**(1):R148–R157.
54. Shen J, *et al*. Development of activity in the mouse visual cortex. *J Neurosci*. 2016;**36**(48):12259–12275.
55. Gramsbergen A. The development of the EEG in the rat. *Dev Psychobiol*. 1976;**9**(6):501–515.
56. Mirmiran M, *et al*. Neuronal discharge patterns in the occipital cortex of developing rats during active and quiet sleep. *Brain Res*. 1982;**255**(1):37–48.
57. Blumberg MS, *et al*. Dynamics of sleep-wake cyclicity in developing rats. *Proc Natl Acad Sci U S A*. 2005;**102**(41):14860–14864.
58. Seelke AM, *et al*. The microstructure of active and quiet sleep as cortical delta activity emerges in infant rats. *Sleep*. 2008;**31**(5):691–699.
59. Frank MG, *et al*. Development of REM and slow wave sleep in the rat. *Am J Physiol*. 1997;**272**(6 Pt 2):R1792–R1799.
60. Harris KM, *et al*. Dendritic spines of CA 1 pyramidal cells in the rat hippocampus: serial electron microscopy with reference to their biophysical characteristics. *J Neurosci*. 1989;**9**(8):2982–2997.
61. Hruska M, *et al*. Synaptic nanomodules underlie the organization and plasticity of spine synapses. *Nat Neurosci*. 2018;**21**(5):671–682.
62. Katz Y, *et al*. Synapse distribution suggests a two-stage model of dendritic integration in CA1 pyramidal neurons. *Neuron*. 2009;**63**(2):171–177.
63. Nusser Z, *et al*. Cell type and pathway dependence of synaptic AMPA receptor number and variability in the hippocampus. *Neuron*. 1998;**21**(3):545–559.
64. Matsuzaki M, *et al*. Dendritic spine geometry is critical for AMPA receptor expression in hippocampal CA1 pyramidal neurons. *Nat Neurosci*. 2001;**4**(11):1086–1092.
65. Makino H, *et al*. Compartmentalized versus global synaptic plasticity on dendrites controlled by experience. *Neuron*. 2011;**72**(6):1001–1011.
66. Hayashi-Takagi A, *et al*. Labelling and optical erasure of synaptic memory traces in the motor cortex. *Nature*. 2015;**525**(7569):333–338.
67. Mattson MP, *et al*. Intermittent metabolic switching, neuroplasticity and brain health. *Nat Rev Neurosci*. 2018;**19**(2):63–80.
68. Blanquie O, Yang JW, Kilb W, Sharopov S, Sinning A, Luhmann HJ. Electrical activity controls area-specific expression of neuronal apoptosis in the mouse developing cerebral cortex. *Elife*. 2017;**6**. pii:e27696. doi:10.7554/eLife.27696
69. Sanes JR, *et al*. Many paths to synaptic specificity. *Annu Rev Cell Dev Biol*. 2009;**25**:161–195.